Journal of Materials Chemistry

Cite this: J. Mater. Chem., 2012, 22, 8367

www.rsc.org/materials

PAPER

Electroactive and biocompatible hydroxyl- functionalized graphene by ball milling

Lu Yan,[a] Mimi Lin,[a] Chao Zeng,[a] Zhi Chen,[a] Shu Zhang,[a] Xinmei Zhao,[b] Aiguo Wu,[b] Yaping Wang,[a] Liming Dai,*[ac] Jia Qu,*[a] Mingming Guo[d] and Yong Liu*[a]

Received 16th February 2012, Accepted 28th February 2012
DOI: 10.1039/c2jm30961k

Hydroxyl-functionalized graphene (G–OH) was efficiently produced from exfoliation of graphite powder by ball milling the presence of potassium hydroxide (KOH). While the nanoscale graphene sheets were confirmed by various characterization techniques, including atomic force microscopy (AFM), scanning electron microscopy (SEM), transmission electron microscopy (TEM), and UV-vis spectroscopy, the formation of hydroxyl groups in G–OH was revealed by Fourier transform infrared (FTIR), Nuclear Magnetic Resonance analysis (NMR), Raman and X-ray photoelectron spectroscopic (XPS) measurements. The as-prepared G–OH showed strong hydrophilicity with good solubility in water, excellent electrochemical activity and no influence on the growth of human retinal pigment epithelium (RPE) cells. More than 80% cell survival rate and less than 7% lactate dehydrogenase (LDH) release were observed for RPE cells treated with G–OH, indicating excellent biocompatibility.

1. Introduction

Owing to its wide range of potential applications,[1–8] graphene has attracted ever increasing attention. As a consequence, various preparation techniques, including mechanical exfoliation of graphite,[1] chemical exfoliation of graphite,[9,10] epitaxial growth on silicon carbide or metal substrates using chemical vapor deposition (CVD),[5,11–13] and zipping carbon nanotubes,[14,15] have been developed. Among them, mechanical exfoliation and CVD are considered to be inapplicable to large-scale production due to the size limitation intrinsically associated with these two methods. Although chemical exfoliation of graphite by acid oxidation in water could allow for large-scale production of graphene nanosheets, the solution exfoliation method suffers many drawbacks, including a complicated preparation process, tedious acid/H_2O removal, and poor product quality. Furthermore, the presence of different oxygen-containing groups (*e.g.*, hydroxyl, carboxyl, epoxy) on the acid-oxidized graphene sheets often makes subsequent functionalization complicated and uncontrollable.[16–18] It may also cause detrimental effects on graphene properties, for example, leading to low conductivity, structural defects, and poor thermal and mechanical stabilities. In this communication, we report a facile, but efficient and versatile, technique for preparing hydroxyl-functionalized graphene (G–OH) by ball milling in the presence of KOH. Knieke *et al.* and Zhao *et al.* have demonstrated the preparation of graphene using a wet ball milling technique.[19,20] Graphite layers were vigorously exfoliated by means of mechanical shear forces. Apart from this, we used solid KOH powder and graphite flakes to prepare G–OH in one step using ball milling in the solid state. The exfoliation of graphite layers could be achieved by both shear forces and the formation of –OH groups on the graphite layer from the solid-state mechanochemical reaction. No graphene nanosheet was obtained without the addition of KOH. The resulting G–OH was thus found to have better water solubility and quality than graphene prepared from wet ball milling due to the presence of –OH. As we shall see later, the resultant G–OH nanosheets also showed good hydrophilicity, excellent electroactivity and biocompatibility with human RPE cells.

2. Experimental

2.1. Materials and reagents

Graphite flakes were provided by Qingdao Haida Corporation. KOH was supplied by Sigma-Aldrich. Dulbecco's Modified Eagle's Medium (DMEM), Fetal Bovine Serum (FBS), and trypsin were all purchased from Invitrogen Corporation. A Cell Counting Kit-8 (CCK-8) was obtained from Dojindo Molecular Technologies, Inc. A Lactate Dehydrogenase (LDH) Release Test Kit (CytoTox 96® Non-Radioactive Cytotoxicity Assay) was obtained from Promega Corporation. A Hoechst Staining

[a]*Institute of Advanced Materials for Nano-Bio Applications, School of Ophthalmology & Optometry, Wenzhou Medical College, 270 Xueyuan Xi Road, Wenzhou, Zhejiang 325027, China. E-mail: jia.qu@163.com; liming.dai@case.edu; yongliu1980@hotmail.com*
[b]*Ningbo Institute of Materials Technology of Engineering (NIMTE), Chinese Academy of Sciences, 519 Zhuangshi Da Dao, Ningbo, Zhejiang 315201, China*
[c]*Department of Macromolecular Science and Engineering, Case Western Reserve University, Cleveland, Ohio 44106, USA*
[d]*Polymer Science Institute, University of Akron, Akron, Ohio, 44325, USA*

Kit was supplied by Beyotime Biotechnology. All other chemicals were purchased from Sigma-Aldrich.

2.2. Preparation of hydroxyl–graphene (G–OH)

G–OH was prepared from naturally crystalline graphite flakes using a ball milling method. Typically, 10 mg graphite and 200 mg potassium hydroxide were mixed in an agate capsule containing a milling ball. The capsule was vigorously shaken at a rate of 200 rpm for 8 h in air at room temperature using a planetary ball mill. The resulting mixture was subsequently removed from the capsule using 15 ml deionized (DI) water. The mixture was immediately centrifuged at 2 000 rpm for 20 min. The upper layer remained and was transferred to a dialysis bag which was pretreated in boiling water for 10 min, followed by soaking in DI water to remove ions. The deionized water was changed every 10 min to completely remove all impurities. The above procedure was repeated three times to ensure that all impurities were removed.

2.3. Electrochemical measurements

Cyclic voltammograms were conducted in a divided three-electrode cell controlled by a CHI 760D (CH Instrument) bipotentiostat. An Ag/AgCl reference and a Pt wire auxiliary electrode were used respectively throughout the work. One drop of G–OH and GO were coated onto a GC disk electrode (i.d. 3 mm), respectively. The electrodes were dried in air prior to electrochemical characterisation. The potential was cycled from −0.3 V to +0.8 V (*vs.* Ag/AgCl) at a scan rate of 0.05 V s^{-1} in an aqueous solution of 10 mM $K_4Fe(CN)_6$/0.1 M $NaNO_3$.

2.4. Cell culturing

5000 cells $well^{-1}$ ARPE-19 cells were seeded in 96-well plates containing DMEM/F12 medium and 10% FBS. Cells were cultured in the incubator for 24, 48, 72 h, respectively, with the addition of various amounts of G–OH. Cells cultured in the medium without G–OH were used as a control. All ARPE-19 cells were cultured at 37 °C in a 95% air/5% CO_2 humidified incubator.

3. Results and discussion

Solid-phase mechanochemical reactions involve highly reactive centers generated by the mechanical energy imparted to the reaction system (*e.g.*, ball milling). Wang *et al.* reported the preparation of dumbbell-shaped C_{120} from C_{60} and potassium cyanide or potassium hydroxide by means of nucleophilic addition.[21] Zhang *et al.* discovered the synthesis of [60]fullerols from the solid-state mechanochemical reaction of [60]fullerene and KOH in air. The nucleophilic attack of hydroxide on the [60]fullerene was found to be essential for the formation of fullerols.[22] We have previously used the ball milling technique to prepare carbon nanotubes functionalized with multiple hydroxyl groups (carbon nanotubols) for self-assembling.[23] In the present study, we mixed graphite and KOH at a weight ratio of 1 : 20 (W_G/W_{KOH}) in an agate capsule with a milling ball. Using a planetary ball milling unit, the capsule was vigorously shaken for several hours at a rate of 200 rpm in air at room temperature. As shown schematically in Fig. 1a, graphite powder could be mechanically exfoliated into G–OH sheets during ball milling in the presence of KOH.[13,14] The nucleophilic attack of hydroxide on the layered graphite and the vigorous shaking will facilitate the exfoliation of graphite and formation of hydroxyl groups through a method similar to those described in the preparation of [60]fullerols[22] and hydroxyl–carbon nanotubes.[23]

The resultant G–OH thus prepared was found to disperse well in water (right, Fig. 1b). In a control experiment, we carried out the ball milling of graphite under the same conditions, but without the incorporation of KOH. As can be seen in Fig. 1b (left), the black powder produced by ball milling without KOH could only partially disperse in water, suggesting that the solid-phase mechanochemical reaction is essential for the formation of water-soluble G–OH. The strong hydrophilicity of G–OH was further evident by contact angle measurements on a CD plate (Dataphysics Model OCA15EC) before and after deposition of the G–OH. As shown in Fig. 1c (top), the pristine CD substrate showed an air–water contact angle of 105°. By contrast, the corresponding contact angle for the G–OH deposited CD plate was found to be 30° (bottom, Fig. 1c), indicating a significant hydrophilicity enhancement due to the presence of hydroxyl groups in the G–OH (*vide infra*).

Fig. 1d shows an AFM image in tapping mode for the as-synthesized G–OH nanosheets deposited from a dilute solution onto a Si substrate. While μm-size graphene sheets are clearly seen in the AFM image, the corresponding height profile shows an average thickness of ~1 nm for the resultant G–OH, suggesting that the G–OH film consists of single- to a few-layer graphene sheets.[5,24,25] The corresponding SEM image given in Fig. 1e shows a similar feature to Fig. 1d for homogeneously dispersed G–OH nanosheets, indicating, once again, the good exfoliation of graphite by mechanical ball milling. Fig. 1f shows

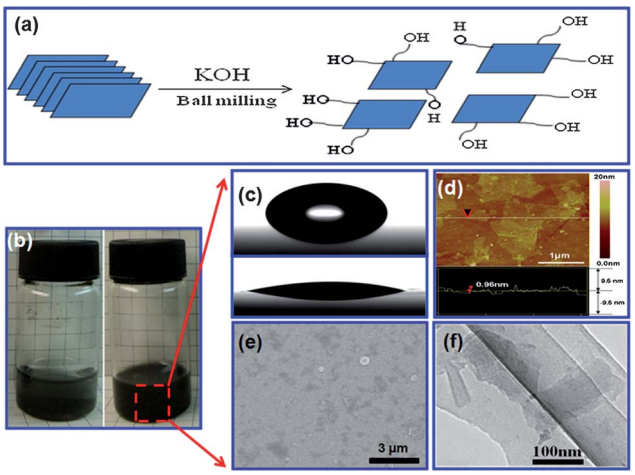

Fig. 1 (a) Schematic of the synthesis of G–OH *via* ball milling. (b) Digital camera image of (right) the G–OH obtained from ball milling with KOH dissolved in DI water and (left) the corresponding sample obtained from ball milling without KOH dispersed in water. (c) Water contact angle of (top) a CD plate and (bottom) the same CD plate after depositing G–OH obtained from ball milling with KOH. (d) AFM micrograph of G–OH, along with its height profile. (e) SEM micrograph of G–OH on a Si substrate. (f) TEM micrograph of G–OH on a TEM grid.

a TEM image of the dispersed G–OH, which clearly reveals monolayer graphene overlapped with a few smaller sheets.

Further evidence for the presence of hydroxyl groups in G–OH comes from Fourier transform infrared (FTIR), Nuclear Magnetic Resonance analysis (NMR) and X-ray photoelectron spectroscopic (XPS) measurements. As shown in Fig. 2a, the hydroxyl IR bands (~3400 cm^{-1}), along with those due to ester (~1000 cm^{-1}) and carbonyl groups (~1700 cm^{-1}) appeared upon ball milling of graphite in the presence of KOH whereas no such bands were found in the corresponding FTIR spectrum of graphite. Comparing to the stretching vibration modes of esters (~1000 cm^{-1}) and carbonyls (~1700 cm^{-1}), the intensity of the hydroxyl band (~3400 cm^{-1}) increased significantly with increasing amounts of KOH introduced into the ball milling system, indicating a preferential introduction of the hydroxyl groups over other oxygen-containing functionalities.

A solid-state Magic Angle Spinning (MAS) NMR analysis of G–OH was performed using a Varian VNMR 500 MHz NMR spectrometer (^1H frequency) operating at 125.62 MHz. The dried powder sample was packed into 4 mm Si nitride rotors with PTFE end caps spinning at 10 kHz. The ^{13}C NMR spectrum of G–OH is shown in Fig. 2b. The typical resonance at 121 ppm is associated with the sp^2-hybridized carbon.[26–28] Peaks at 100 ppm and 72 ppm are assigned as the lactol[29] and hydroxyl groups[28,29] respectively, conforming the presence of hydroxyl groups. The peak at 116 ppm is due to the PTFE end caps of the solid-state NMR rotor.[27]

XPS spectroscopic measurements on G–OH further confirms the predominate presence of hydroxyl groups. As expected, the survey spectrum given in Fig. 2c shows only the C and O peaks for G–OH. Fig. 2d reproduces the high-resolution C 1s spectrum for G–OH, which exhibits the presence of C–C (284.8 eV), C–O (285.5 eV) and C–O–C (286.8 eV) groups respectively. The XPS results are consistent with the FTIR and NMR results.

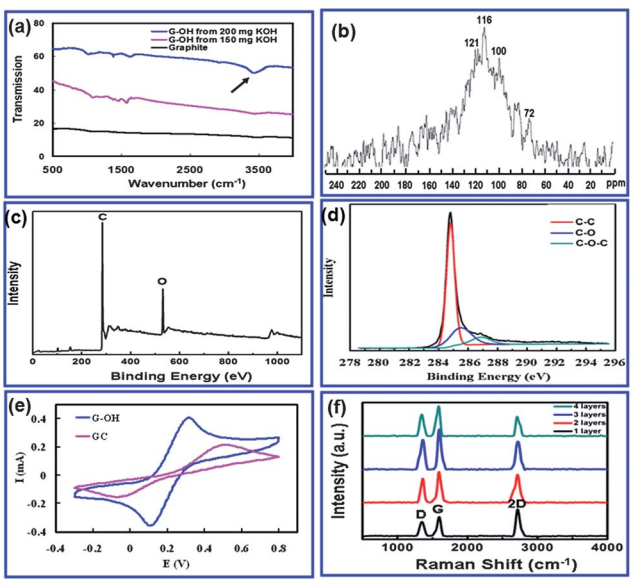

Fig. 2 (a) FTIR spectrum of G–OH compared with that of pristine graphite. (b) Solid-state ^{13}C MAS NMR spectrum (125.62 MHz, 10 kHz MAS) of G–OH; (c) XPS survey spectrum of the resultant G–OH. (d) High-resolution XPS C 1s spectrum of the G–OH; (e) CVs of GC and G–OH on GC; and (f) Raman spectra of G–OH with various layer numbers.

We further studied the electrochemical properties of the G–OH. Fig. 2e shows CVs of the G–OH coated glassy carbon (GC) (blue line) and the pristine GC (pink line) in 10 mM $K_4F(CN)_6$/0.1 M $NaNO_3$, respectively. One stable redox couple at +0.315 V and 0.107 V assigned to the $[Fe(CN)_6]^{4-}/[Fe(CN)_6]^{3-}$ redox pair were observed for the G–OH while redox peaks were found at +0.518 V and −0.078 V for the pristine GC. The peak separation (ΔE) significantly decreased from 0.596 V to 0.208 V when the G–OH was introduced onto the GC, suggesting that the electron transfer rate was significantly faster on the G–OH than that on the GC. Much higher peak currents were obtained for the G–OH, indicating that the G–OH had a higher surface area than the GC. Electrochemical measurement suggests the good electroactivity of the G–OH.

To investigate the graphitization degree of the G–OH, we further performed Raman spectroscopic measurements. Raman spectra of the as-synthesized G–OH sheets with different layer numbers are given in Fig. 2f, which shows three peaks characteristic of the D band (~ 1357 cm^{-1}, sp^3 carbon), G band (~1585 cm^{-1}, sp^2 carbon), and 2D band (~2726 cm^{-1}) with the intensity ratio of the 2D to G band being sensitive to the layer number. The peak intensity ratio of the D to G band (I_D/I_G ~ 0.5) is slightly higher than the corresponding ratio for the nitrogen-doped graphene (N-graphene) that we reported earlier,[5,30] indicating the introduction of a significant amount of hydroxyl groups into the graphene lattice led to an obvious increase in the amount of sp^3 carbon.[31] The shape of the 2D band and the intensity ratio of the G band to the 2D band (I_G/I_{2D}) are proven to be sensitive to the number of graphene layers as shown in Fig. 2f.[32,33] I_G/I_{2D} increased from 0.73 to 1.55 when the layer number of graphene increased from 1 layer to 4 layers. For comparison, the relatively high ratio of I_D/I_G for the G–OH with respect to N-graphene[5] indicates that ball milling in the presence of KOH introduces relatively a high percentage of hydroxyl groups, consistent with the XPS results. The presence of a large amount of hydroxyl groups could significantly enhance the hydrophilicity of graphene and provide additional advantages for the G–OH to be used in biomedical systems. In this context, we further investigated the biocompatibility of the as-synthesized G–OH with human RPE cells.

ARPE-19, a cell line derived from human RPE was cultured in culture media mixed with various amount of G–OH. We found that the cell morphology remained the same with the addition of G–OH. No visible change was observed when RPE cells were cultured without (Fig. 3a) or with (Fig. 3b) addition of 100 μg ml^{-1} G–OH for 72 h, suggesting low toxicity of G–OH to the growth and proliferation of ARPE-19 cells. This was further confirmed by a cell survival rate assay using a Cell Counting Kit-8 (CCK-8) assay.[34] The cell viability in G–OH containing solution was found to be higher than 80% even after 4 days' culturing (Fig. 3c), indicating excellent biocompatibility of G–OH. There is no obvious decrease in cell survival rate with increasing G–OH content from 5 μg ml^{-1} to 100 μg ml^{-1}. We further carried out an apoptotic study of ARPE-19 cells induced by 100 μg ml^{-1} G–OH. APRE-19 cells with 100 μg ml^{-1} G–OH were incubated for 72 h prior to being harvested and washed using phosphate buffer solution (PBS) (pH 7.4). Cells were subsequently fixed by fixatives and stained by Hoechst 33258 to be observed by fluorescence microscopy (Zeiss, Germany).[35] As shown in Fig. 3d,

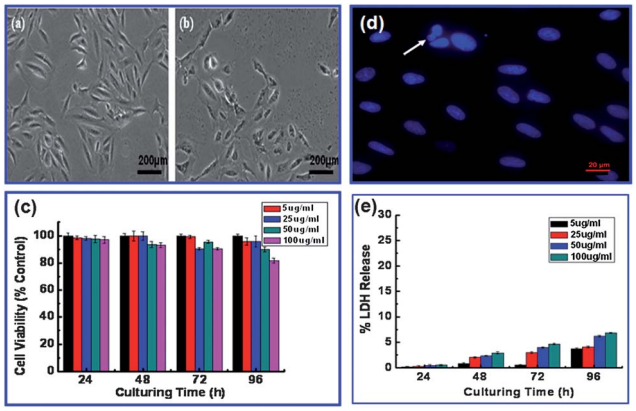

Fig. 3 Optical micrograph of ARPE-19 cells after 72 h incubation (a) without G–OH (the control) and (b) with 100 μg ml^{-1} G–OH; (c) cell survival rate assay of ARPE-19 cells incubated with 0 μg ml^{-1} (black), 5 μg ml^{-1} (red), 25 μg ml^{-1} (blue), 50 μg ml^{-1} (green) and 100 μg ml^{-1} (pink) G–OH for 24, 48, 72 and 96 h, respectively; (d) fluorescence micrograph of Hoechst 33258 stained ARPE-19 cells incubated with 100 μg ml^{-1} G–OH (white arrow indicates cell apoptosis); and (e) LDH assay for detection of ARPE-19 cells incubated with 5 μg ml^{-1} (black), 25 μg ml^{-1} (red), 50 μg ml^{-1} (blue), and 100 μg ml^{-1} (green) G–OH after 24, 48, 72 and 96 h incubation, respectively.

apoptotic cells (white arrow in Fig. 3d) are round in shape. An enhanced fluorescence signal and condensed nucleus were also observed in apoptotic cells. These results suggest that G–OH did induce some apoptosis or necrosis. We further studied the LDH release level[34] of ARPE-19 cells with G–OH to measure the cell membrane integrity. Fig. 3e shows that the LDH release with various amounts of G–OH (up to 100 μg ml^{-1}) was less than 7% in all cases, suggesting the good biocompatibility of G–OH with ARPE-19 cells. The LDH result is consistent with the cell survival rate assay.

Conclusions

We have developed a simple and efficient method for the preparation of hydroxyl-functionalized graphene by ball milling in the presence of KOH. The resultant G–OH is highly electroactive, hydrophilic and water soluble. While AFM, SEM, TEM and Raman have been used to confirm the presence of single to a few layer G–OH sheets, the successful introduction of –OH groups on graphene was evident by FTIR and XPS measurements. The as-prepared G–OH exhibited good biocompatibility with human RPE cells. RPE cells showed higher than 80% cell viability by CCK-8 assay in G–OH solutions and less than 7% LDH release, though a small amount of apoptosis was observed. The facile and efficient fabrication of electroactive and biocompatible G–OH directly by simple ball milling opens up possibilities for the large-scale production of functionalized graphene nanosheets for various applications, especially in biological and biomedical systems.

Acknowledgements

The authors are grateful to Dr Ling Hou (Wenzhou Medical College) for kindly providing the ARPE-19 cells. Financial support from the Chinese National Nature Science Foundation (81000663), the Ministry of Education of China (211069, IRT1077), the National "Thousand Talents Program", the Ministry of Science and Technology of China (2009DFB30380), Doctoral Fund of Ministry of Education of China (20103321120003), the Zhejiang Department of Science and Technology (2009C13019), the Zhejiang Department of Education (Y200906587) and the Ningbo Natural Science Foundation of China (2011A610140) are acknowledged.

References

1 K. S. Novoselov, A. K. Geim, S. V. Morozov, D. Jiang, Y. Zhang, S. V. Dubonos, I. V. Grigorieva and A. A. Firsov, *Science*, 2004, **306**, 666.
2 X. Wang, L. J. Zhi and K. Mullen, *Nano Lett.*, 2008, **8**, 323.
3 Y. M. Lin, C. Dimitrakopoulos, K. A. Jenkins, D. B. Farmer, H. Y. Chiu and A. Grill, *Science*, 2010, **327**, 662.
4 S. Stankovich, D. A. Dikin, G. H. B. Dommett, K. M. Kohlhaas, E. J. Zimney, E. A. Stach, R. D. Piner, S. T. Nguyen and R. S. Ruoff, *Nature*, 2006, **442**, 282.
5 L. Qu, Y. Liu, J. B. Baek and L. Dai, *ACS Nano*, 2010, **4**, 1321.
6 Y. Liu, D. Yu, C. Zeng, Z. Miao and L. Dai, *Langmuir*, 2010, **26**, 6158.
7 A. K. Geim and K. S. Novoselov, *Nat. Mater.*, 2007, **6**, 183.
8 H. Chen, M. B. Müller, K. J. Gilmore, G. G. Wallce and D. Li, *Adv. Mater.*, 2008, **20**, 3557.
9 S. Stankovich, D. A. Dikin, R. D. Piner, K. A. Kohlhaas, A. Kleinhammes, Y. Jia, Y. Wu, S. T. Nguyen and R. S. Ruoff, *Carbon*, 2007, **45**, 1558.
10 D. Li, M. B. Müller, S. Gilje, R. B. Kaner and G. G. Wallace, *Nat. Nanotechnol.*, 2008, **3**, 101.
11 P. Sutter, *Nat. Mater.*, 2009, **8**, 171.
12 S. Bae, H. Kim, Y. Lee, X. Xu, J. Park, Y. Zheng, J. Balakrishnan, T. Lei, H. R. Kim, Y. I. Song, Y. J. Kim, K. S. Kim, B. Özyilmaz, J. H. Ahn, B. H. Hong and S. Iijima, *Nat. Nanotechnol.*, 2010, **5**, 574.
13 X. Li, W. Cai, J. An, S. Kim, J. Nah, D. Yang, R. Piner, A. Velamakanni, I. Jung, E. Tutuc, S. K. Banerjee, L. Columbo and R. S. Ruoff, *Science*, 2009, **324**, 1312.
14 L. Jiao, L. Zhang, X. Wang, G. Diankov and H. Dai, *Nature*, 2009, **458**, 877.
15 D. V. Kosynkin, A. L. Higginbotham, A. Sinitskii, J. R. Lomeda, A. Dimiev, B. K. Price and J. M. Tour, *Nature*, 2009, **458**, 872.
16 S. Stankovicha, S. T. Nguyenb and R. S. Ruoffa, *Carbon*, 2006, **44**, 3342.
17 R. Muszynski, B. Seger and P. V. Kamat, *J. Phys. Chem.*, 2008, **112**, 5263.
18 K. Tanaka and F. Toda, *Chem. Rev.*, 2000, **100**, 1025.
19 C. Knieke, A. Berger, M. Voigt, R. N. K. Taylor, J. Rohrl and W. Peukert, *Carbon*, 2010, **48**, 3196.
20 W. Zhao, M. Fang, F. Wu, H. Wu, L. Wang and G. Chen, *J. Mater. Chem.*, 2010, **20**, 5817.
21 G. Wang, K. Komatsu, Y. Murata and M. Shiro, *Nature*, 1997, **387**, 583.
22 P. Zhang, H. Pan, D. Liu, Z. Guo, F. Zhang and D. Zhu, *Synth. Commun.*, 2003, **33**, 2469.
23 H. Pan, L. Liu, Z. Guo, L. Dai, F. Zhang, D. Zhu, R. Czerw and D. L. Carrol, *Nano Lett.*, 2003, **3**, 29.
24 V. C. Tung, M. J. Allen, Y. Yang and R. B. Kaner, *Nat. Nanotechnol.*, 2009, **4**, 25.
25 X. Li, G. Zhang, X. Bai, X. Sun, X. Wang, E. Wang and H. Dai, *Nat. Nanotechnol.*, 2008, **3**, 538.
26 Y. Si and E. T. Samulski, *Nano Lett.*, 2008, **8**, 1679.
27 Y. Xue, H. Chen, D. Yu, S. Wang, M. Yardeni, Q. Dai, M. Guo, Y. Liu, F. Lu, J. Qu and L. Dai, *Chem. Commun.*, 2011, **47**, 11689.
28 H. Jeong, Y. P. Lee, R. J. W. E. Lahaye, M. Park, K. H. An, I. J. Kim, C. Yang, C. Y. Park, R. S. Ruoff and Y. H. Lee, *J. Am. Chem. Soc.*, 2008, **130**, 1362.
29 W. Gao, L. B. Alemany, L. Ci and P. M. Ajayan, *Nat. Chem.*, 2009, **1**, 403.
30 A. C. Ferrari, *Solid State Commun.*, 2007, **143**, 47.

31 L. S. Panchokarla, K. S. Subrahmanyam, S. K. Saha, A. Govindaraj, H. R. Krishnamurthy, U. V. Waghmare and C. N. R. Rao, *Adv. Mater.*, 2009, **21**, 4726.
32 K. S. Kim, Y. Zhao, H. Jang, S. Y. Lee, J. M. Kim, K. S. Kim, J. H. Ahn, P. Kim, J. Y. Choi and B. H. Hong, *Nature*, 2009, **457**, 706.
33 A. Reina, X. Jia, J. Ho, D. Nezich, H. Son, V. Bulovic, M. S. Dresselhaus and J. Kong, *Nano Lett.*, 2009, **9**, 30.
34 R. Hamamoto, Y. Furukawa, M. Morita, Y. Iimura, F. P. Silva, M. Li, R. Yagyu and Y. Nakamura, *Nat. Cell Biol.*, 2004, **6**, 731.
35 R. K. Srivastava, A. B. Pant, M. P. Kashyap, V. Kumar, M. Lohani, L. Jonas and Q. Rahman, *Nanotoxicology*, 2011, **5**, 195.